Inorg. Chem. **2008**, *47*, 9333−9343

Solid- and Solution Phase Transformations in Novel Hybrid Iodoplumbate Derivatives Templated by Solvated Yttrium Complexes

Shashank Mishra,*,† Erwann Jeanneau,‡ Stéphane Daniele,*,† Gilles Ledoux,§ and Prakash N. Swamy†

IRCELYON, Université Lyon 1, 2 Avenue A. Einstein, 69626 Villeurbanne, France, Centre de Diffractométrie, Université Lyon 1, 69622 Villeurbanne, France, Laboratoire de Physico Chimie des Matériaux Luminescent, Université Lyon 1, CNRS UMR 5620, 10 rue A. M. Ampère, 69622 Villeurbanne, France

Received June 5, 2008

Solvated yttrium iodide precursors $[Y(L)_8]I_3$ [L = dimethylformamide (DMF) or dimethylsulfoxide (DMSO)], prepared in situ by stirring $YI_3(Pr^iOH)_4$ in DMF/DMSO, react with 3 equiv of PbI_2 in the presence of NH_4I to give novel hybrid derivatives based on either a one-dimensional (1D) straight chain, $[Y(DMF)_8][Pb_3(\mu\text{-}I)_9]_{1\infty}\cdot DMF$ (**1**), or discrete pentanuclear iodoplumbates, $[Y(DMSO)_8]_2[(DMSO)_2Pb_5(\mu_3\text{-}I)_2(\mu\text{-}I)_8I_6]$ (**2a**). The complex **2a** and a closely related $[Y(DMSO)_8][Y(DMSO)_7(DMF)][(DMSO)_2Pb_5(\mu_3\text{-}I)_2(\mu\text{-}I)_8I_6]$ (**2b**) were obtained in good yield by solution phase transformation of **1** in DMSO under slight different conditions. Derivatives **1** and **2** also undergo unique solid-state transformation in a confined environment of paratone to give 1D polymers based on zigzag iodoplumbate chains; crystals of **1** transform into $[Y(DMF)_6(H_2O)_2][Pb_3(\mu_3\text{-}I)(\mu\text{-}I)_7I]_{1\infty}$ (**3**) via an exchange reaction, whereas those of **2a** and **2b** are converted into $[Y(DMSO)_7][Pb_3(\mu_3\text{-}I)(\mu\text{-}I)_7I]_{1\infty}$ (**4**) via a decomposition pathway. The trifurcate H-bonding between water ligands on yttrium cation and iodide of the iodoplumbate anion plays a pivotal role in transforming the straight 1D polymeric Pb−I chain of **1** into a zigzag chain in **3**. The thermogravimetry-differential thermal analysis studies indicate that complexes with DMF ligands are thermally more stable than those with DMSO ones, the mixed DMF-H_2O ligand complex **3** being the most stable one because of the presence of strong H-bonding. Diffuse-reflectance UV−visible spectral analyses of **1**−**4** show an optical band gap in the 1.86−2.54 eV range, indicating these derivatives as potential semiconductors. In contrast to non-emissive **3** and **4**, derivatives **1**, **2a**, and **2b** show remarkable luminescent emission with peak maxima at 703 nm, assigned as an iodine 5p-lead 6s to lead 6p charge transfer (XM-M-CT).

Introduction

Hybrid organic−inorganic molecular compounds have recently developed into an important class of solid-state materials,[1] owing to their enormous variety of intriguing structural topologies and fascinating properties, as well as potential applications in many fields such as catalysis, materials science, magnetochemistry, and medicine.[2] These compounds containing metal halides as an inorganic moiety constitute an important family of hybrid functional materials,[3] among which lead(II) iodide

* To whom correspondence should be addressed. E-mail: mishrashashank74@rediffmail.com. Phone: +33 472445329. Fax: +33 472445399.

† IRCELYON.

‡ Centre de Diffractométrie.

§ Laboratoire de Physico Chimie des Matériaux Luminescent.

(1) Cheetham, A. K.; Rao, C. N. R. *Science* **2007**, *318*, 58–59.

(2) (a) Niu, Y.-Y.; Zheng, H.-G.; Hou, H.-W.; Xin, X.-Q. *Coord. Chem. Rev.* **2004**, *248*, 169–183. (b) Wu, C.-D.; Lu, C.-Z.; Lin, X.; Wu, D.-M.; Lu, S.-F.; Zhuang, H.-H.; Huang, J.-S. *Chem. Commun.* **2003**, 1284–1285. (c) Yaghi, O. M.; Li, H.; Davis, C.; Richardson, D.; Groy, T. L. *Acc. Chem. Res.* **1998**, *31*, 474–484. (d) Cheetham, A. K. *Science* **1994**, *264*, 794–795.

(3) (a) Arnby, C. H.; Jagner, S.; Dance, I. *CrystEngComm* **2004**, *6*, 257–275. (b) Papavassiliou, G. C.; Mousdis, G. A.; Koutselas, I. B. *Adv. Mater. Opt. Electron.* **1999**, *9*, 265–271. (c) Papavassiliou, G. C. *Prog. Solid State Chem.* **1997**, *25*, 125–270. (d) Mitzi, D. B.; Feild, C. A.; Harrison, W. T. A.; Guloy, A. M. *Nature* **1994**, *369*, 467–469.

(4) (a) Sourisseau, S.; Louvain, N.; Bi, W.; Mercier, N.; Rondeau, D.; Boucher, F.; Buzare, J.-Y.; Legein, C. *Chem. Mater.* **2007**, *19*, 600–607. (b) Zhang, Z.-J.; Xiang, S.-C.; Zhang, Y.-F.; Wu, A.-Q.; Cai, L.-Z.; Guo, G.-C.; Huang, J.-S. *Inorg. Chem.* **2006**, *45*, 1972–1977. (c) Zhang, Z.-J.; Guo, G.-C.; Xu, G.; Fu, M.-L.; Zou, J.-P.; Huang, J.-S. *Inorg. Chem.* **2006**, *45*, 10028–10030. (d) Glavcheva, Z.; Umezawa, H.; Okada, S.; Nakanishi, H. *Mater. Lett.* **2004**, *58*, 2466–2471. (e) Guloy, A. M.; Tang, Z.-J.; Miranda, P. B.; Srdanov, V. I. *Adv. Mater.* **2001**, *13*, 833–837. (f) Mousdis, G. A.; Gionis, V.; Papavassilliou, G. C.; Raptopoulou, C. P.; Terzis, A. *J. Mater. Chem.* **1998**, *8*, 2259–2262. (g) Mitzi, D. B.; Wang, S.; Feild, C. A.; Chess, C. A.; Guloy, A. M. *Science* **1995**, *267*, 1473–1476.

10.1021/ic8010376 CCC: $40.75
Published on Web 09/23/2008

organic−inorganic hybrid complexes have received special attention for their tunable structural and physical properties, in particular their intriguing optical and semiconducting ones.[4] For these materials, the structure and dimensionality of the iodoplumbate anion is extremely sensitive to the specific reaction conditions and counter cations used.[5] A large variety of compositions of iodoplumbates including $Pb_3I_9^{3-}$, $Pb_3I_{10}^{4-}$, $Pb_3I_{11}^{5-}$, $Pb_5I_{12}^{2-}$, $Pb_5I_{18}^{8-}$, $Pb_7I_{18}^{4-}$, $Pb_{10}I_{28}^{8-}$, $Pb_{15}I_{34}^{4-}$, and $Pb_{18}I_{44}^{8-}$ are known, in which different connectivities of the PbI_6 octahedra via corner, edge-, or face-sharing lead to different structures ranging from isolated anions[6] to infinite chains, layered perovskites, and three-dimensional polymeric networks.[7]

Quite a few inorganic−organic hybrid derivatives based on halometallates have been reported to show solid and/or solution phase transformations. For example, transformation of a zigzag one-dimensional (1D) coordination polymer $[ZnCl_2(\mu\text{-bipy})]_{1\infty}$ to a two-dimensional (2D) network structure $[Zn(\mu\text{-Cl})_2(\mu\text{-bipy})]_{2\infty}$ by cooling below −43 °C and two consecutive reversible phase transitions in a single crystal of $[Pb(\mu\text{-Cl})_2(\mu\text{-bipy})]_{2\infty}$ (bipy = 4,4′-bipyridine), from low-temperature α phase to room temperature intermediate β and finally the maximum symmetry γ phase, have recently been reported.[8] Also, a reversible solid-state transition from a conglomerate to a racemate one at 75 °C has been shown in the hybrid compound $[\{H_3N(CH_2)_2SS(CH_2)_2NH_3\}PbI_5]\cdot H_3O$, the change in the hydrogen bonding at the organic−inorganic interface being the driving force for the transition.[9] Similarly, a 1D polymeric chain of $[Cu_4Br_4(TTT)_2]$ [TTT = triallyl-1,3,5-triazine-2,4,6(1H,3H,5H)-trione] built from Cu_4Br_4 cubanes can be converted to a 2D network $[Cu_6Br_6(TTT)_2]$ consisting of Cu_6Br_6 prisms by reacting the former with CuBr in ethanol,[10] and a red monomeric $[NiBr_2\{P(CH_2CH_2CN)_3\}_2]$ polymerizes on heating the solid at 80−130 °C or in acetone solution to form a blue linear 1D coordination polymer, the solid-state reaction pathway being identical to the solution grown product forming a stereospecific all *trans*-octahedral $NiBr_2P_2N_2$ core from the square-planar $NiBr_2P_2$ core.[11]

Because the choice of a certain cation greatly impacts the structural and physical properties of these metal halide hybrid materials, we decided to incorporate metal-organic cations, instead of the more frequently used organic cations,[5−7] to fine-tune their structural and physical properties by bringing in the properties of a second metal as well. Although some reports describing incorporation of metal-organic in such metal iodide based hybrid materials are available,[6d,7g,12] they mostly deal with transition metal complexes with chelating ligands, that is, $[M(L)_x]^{n+}$ (M = Fe, Co, Ni, Cu, Zn, Ru; L = ethylenediamine, phenanthroline, bipyridine, terpyridine; $x = 2, 3$; $n = 2, 3$).[12] Using $[Ln(L)_x]^{3+}$ (Ln = Y, Tb; L = DMF and/or DMSO; $x = 7, 8$) cation as a templating reagent, we recently succeeded in the synthesis of novel hybrid iodocuperate and iodoargentate complexes with a wide variety of structural architectures ranging from discrete polynuclear complexes to fascinating 1D and 2D networks.[13−15] More interestingly, use of DMF and/or DMSO as coordinating ligands allowed interesting solid-phase transformations by progressive substitution of these monodentate ligands with water molecules, either in a confined environment provided by a paratone medium[13] or under ambient conditions.[14] In this manuscript we wish to report the syntheses and characterization of two novel hybrid iodoplumbate complexes templated by metal-organic complexes, that is, $[Y(DMF)_8][Pb_3I_9]$.DMF (**1**) and $[Y(DMSO)_8]_2[(DMSO)_2Pb_5(\mu_3\text{-}I)_2(\mu\text{-}I)_8I_6]$ (**2a**), which show interesting solution- and solid-phase transformations (Scheme 1). Transformation of **1** in DMSO under slightly different conditions gave two related pentanuclear iodoplumbate based complexes **2a** and $[Y(DMSO)_8][Y(DMSO)_7(DMF)][(DMSO)_2Pb_5(\mu_3\text{-}I)_2(\mu\text{-}I)_8I_6]$ (**2b**). Derivatives **1** and **2** also undergo unique solid-state transformation in a confined, solvent-free environment to give 1D polymers based on zigzag iodoplumbate

(5) (a) Zhu, X.-H.; Mercier, N.; Frere, P.; Blanchard, P.; Roncali, J.; Allain, M.; Pasquier, C.; Riou, A. *Inorg. Chem.* **2003**, *42*, 5330–5339. (b) Krautscheid, H.; Vielsack, F.; Klaassen, N. *Z. Anorg. Allg. Chem.* **1998**, *624*, 807–812.

(6) (a) Zheng, Y.-Y.; Wu, G.; Chen, H.-Z.; Wang, M. *Acta Crystallogr.* **2007**, *E63*, m504–m506. (b) Krautscheid, H.; Vielsack, F. *Z. Anorg. Allg. Chem.* **2000**, *626*, 3–5. (c) Krautscheid, H.; Vielsack, F. *J. Chem. Soc., Dalton Trans.* **1999**, 2731–2735. (d) Krautscheid, H.; Vielsack, F. *Z. Anorg. Allg. Chem.* **1999**, *625*, 562–566. (f) Krautscheid, H.; Vielsack, F. *Angew. Chem., Int. Ed. Engl.* **1995**, *34*, 2035–2037.

(7) (a) Zhang, Z.-J.; Xiang, S.-C.; Guo, G.-C.; Xu, G.; Wang, M.-S.; Zou, J.-P.; Guo, S.-P.; Huang, J.-S. *Angew. Chem., Int. Ed.* **2008**, *47*, 4149–4152. (b) Wang, Y. J.; Li, H. H.; Chen, Z. R.; Huang, C. C.; Huang, X. H.; Feng, M.; Lin, Y. *CrystEngComm* **2008**, *10*, 770–777. (c) Louvain, N.; Bi, W.; Mercier, N.; Buzare, J.-Y.; Legein, C.; Corbel, G. *Dalton Trans.* **2007**, 965–970. (d) Billing, D. G.; Lemmerer, A. *CrystEngComm* **2007**, *9*, 236–244. (e) Billing, D. G.; Lemmerer, A. *Acta Crystallogr.* **2006**, *C62*, m238–m240. (f) Mercier, N. *CrystEngComm* **2005**, *7*, 429–432. (g) Zhu, X.-H.; Mercier, N.; Riou, A.; Blanchard, P.; Frere, P. *Chem. Commun.* **2002**, 2160–2161. (h) Krautscheid, H.; Lode, C.; Vielsack, F.; Vollmer, H. *J. Chem. Soc., Dalton Trans.* **2001**, 1099–1104. (i) Tang, Z.; Guan, J.; Guloy, A. M. *J. Mater. Chem.* **2001**, *11*, 479–482. (j) Tang, Z.; Guloy, A. M. *J. Am. Chem. Soc.* **1999**, *121*, 452–453. (k) Chakravarthy, V.; Guloy, A. M. *Chem. Commun.* **1997**, 697–698. (l) Wang, S.; Mitzi, D. B.; Feild, C. A.; Guloy, A. M. *J. Am. Chem. Soc.* **1995**, *117*, 5297–5302. (m) Louvain, N.; Mercier, N. *Solid State Sci.* [Online early access] DOI: 10.1016/j.solidstatesciences.2007.12.034. Published Online: **2008**.

(8) (a) Hu, C.; Englert, U. *Angew. Chem., Int. Ed.* **2006**, *45*, 3457–3459. (b) Hu, C.; Englert, U. *Angew. Chem., Int. Ed.* **2005**, *44*, 2281–2283.

(9) Mercier, N.; Barres, A. L.; Giffard, M.; Rau, I.; Kajzar, F.; Sahraoui, B. *Angew. Chem., Int. Ed.* **2006**, *45*, 2100–2103.

(10) Xue, X.; Wang, X.-S.; Xiong, R.-G.; You, X. Z.; Abrahams, B. F.; Che, C.-M.; Ju, H.-X. *Angew. Chem., Int. Ed.* **2002**, *41*, 2944–2946.

(11) (a) Cheng, K.; Foxman, B. M. *J. Am. Chem. Soc.* **1977**, *99*, 8102–8103. (b) Walton, R. A.; Whyman, R. *J. Chem. Soc. A* **1968**, 1394–1398. (c) Drew, M. G. B.; Lewis, D. F.; Walton, R. A. *Chem. Commun.* **1969**, 326.

(12) (a) Jiang, Y.-S.; Yao, H.-G.; Ji, S.-H.; Ji, M.; An, Y.-L. *Inorg. Chem.* **2008**, *47*, 3922–3944. (b) Li, H.-H.; Sun, L.-G.; Chen, Z.-R.; Wang, Y.-J.; Li, J.-Q. *Aus. J. Chem.* **2008**, *61*, 391–396. (c) Tershansy, M. A.; Goforth, A. M.; Ellsworth, J. M.; Smith, M. D.; zur Loye, H.-C. *CrystEngComm* **2008**, *10*, 833–838. (d) Tershansy, M. A.; Goforth, A. M.; Peterson, L., Jr.; Burns, M. C.; Smith, M. D.; zur Loye, H.-C. *Solid State Sci.* **2007**, *9*, 895–906. (e) Fan, L.-Q.; Chen, L.; Wu, L.-M. *Acta Crystallogr.* **2006**, *E62*, m3373–m3374. (f) Goforth, A. M.; Gardinier, J. R.; Smith, M. D.; Peterson, L., Jr.; zur Loye, H.-C. *Inorg. Chem. Commun.* **2005**, *8*, 684–688. (g) Yu, J.-H.; Jia, H.-B.; Pan, L.-Y.; Yang, Q.-X.; Wang, T.-G.; Xu, J.-Q.; Cui, X.-B.; Liu, Y.-J.; Li, Y.-Z.; Lu, C.-H.; Ma, T.-H. *J. Solid State Chem.* **2003**, *175*, 152–158.

(13) (a) Mishra, S.; Jeanneau, E.; Chermette, H.; Daniele, S.; Hubert-Pfalzgraf, L. G. *Dalton Trans.* **2008**, 620–630. (b) Mishra, S.; Hubert-Pfalzgraf, L. G.; Jeanneau, E.; Chermette, H. *Dalton Trans.* **2007**, 410–413.

(14) Mishra, S.; Jeanneau, E.; Daniele, S.; Hubert-Pfalzgraf, L. G. *CrystEngComm* **2008**, *10*, 814–816.

(15) Mishra, S.; Jeanneau, E.; Daniele, S.; Ledoux, G. *Dalton Trans.* **2008**, in press; DOI: 10.1039/b809964b.

Scheme 1. Synthesis and Transformations of Novel Hybrid Iodoplumbate Derivatives

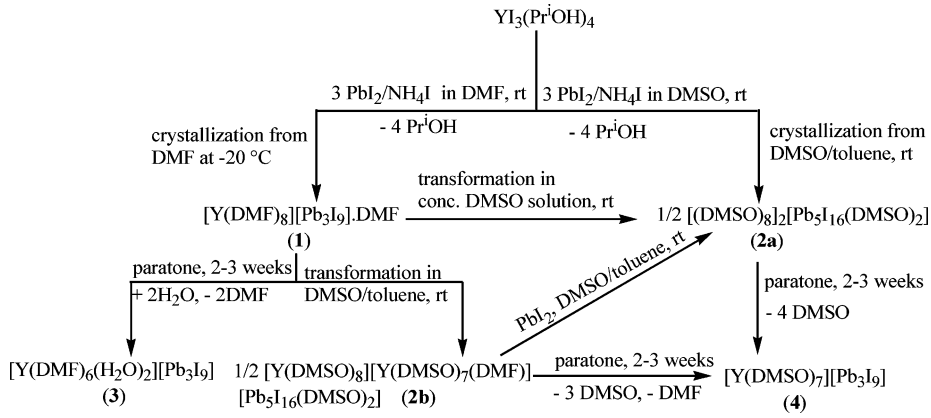

chains. Thus, on leaving in paratone, crystals of **1** transform into $[Y(DMF)_6(H_2O)_2][Pb_3(\mu_3\text{-}I)(\mu\text{-}I)_7I]_{1\infty}$ (**3**) via substitution of two DMF ligands with water molecules, whereas those of **2a** and **2b** are converted into $[Y(DMSO)_7][Pb_3(\mu_3\text{-}I)(\mu\text{-}I)_7I]_{1\infty}$ (**4**) via a decomposition reaction also involving removal of one solvent molecule (DMF and/or DMSO) from the yttrium cation and two DMSO molecules from the $[Pb_5I_{16}(DMSO)_2]^{6-}$ cluster, as well as condensation of this discrete pentanuclear cluster into a zigzag 1D chain. Besides this unique transformation, the work reported here also has some interesting structural features such as a novel discrete $[Pb_5I_{16}(DMSO)_2]^{6-}$ anion in **2** and a new structural motif and isomeric form of 1D iodoplumbate chains in **3** and **4**. In addition, their diffuse-reflectance spectral analyses, thermal and luminescent properties are also reported.

Experimental Section

General Procedures. Although complexes **1**−**4** are stable in air, as a precautionary measure, all manipulations were carried out under argon using Schlenk tubes and vacuum line techniques. PbI_2 (Aldrich) and NH_4I (Sigma-Aldrich) were used as received. $YI_3(Pr^iOH)_4$ was synthesized as described in the literature.[16] Solvents were purified on an MB SPS-800 instrument. ^1H NMR spectra were registered on a Bruker AC-300 spectrometer. FT-IR spectra were recorded as Nujol or paratone mulls on a Perkin-Elmer Paragon 500 spectrometer. Analytical data were obtained from the Service Central d'Analyses du CNRS. Thermogravimetric-differential thermal analysis (TG-DTA) data were collected in air using a Setaram TGA92−12 thermal analyzer (thermal ramp 5 °C/min, temperature range 20−600 °C). The diffuse reflectance spectra of crystalline samples of **1**−**4** (diluted 3 times with SiO_2) were recorded at room temperature from 200 to 700 nm on a Perkin-Elmer Lamda 35 spectrophotometer. X-ray powder patterns of **2a** (before and after calcinations at 140 °C for 2 h) and **4** were obtained with a Bruker (Siemens) D 500 diffractometer using the Cu Kα radiation. Luminescence emission spectra of crystalline samples were recorded at room temperature on a homemade spectrometer using a 450 W xenon arc lamp as the excitation source. The excitation was filtered by a Gemini 180 JobinYvon monochromator with 2 mm slits ensuring an excitation resolution of 4 nm, and the luminescence was collected by an optical fiber coupled with a TRIAX320 Jobin Yvon monochromator. Light was then detected by a Peltier cooled CCD camera. The resolution used in emission was 1.5 nm.

(16) Mishra, S.; Hubert-Pfalzgraf, L. G.; Rolland, M.; Chermette, H. *Inorg. Chem. Commun.* **2007**, *10*, 15–19.

Synthesis of 1−4. $[Y(DMF)_8][Pb_3(\mu\text{-}I)_9]_{1\infty}\cdot DMF$ (1). The DMF solution of NH_4I (2 mL, 3.5 M) was added dropwise to a suspension of PbI_2 (1.62 g, 2.78 mmol) in 3 mL of DMF, giving a clear yellow solution. This solution was transferred to a prestirred suspension of $YI_3(Pr^iOH)_4$ (0.66 g, 0.93 mmol) in 5 mL of DMF. After stirring for 2 h at room temperature, the yellow solution obtained was concentrated up to 5 mL. Pale-yellow plate-like crystals of **1** grew overnight at −20 °C and were separated by decanting. One more crop of crystals was obtained from the concentrated mother liquid. Yield, 1.79 g (77%). Anal. Found: C, 12.86; H, 2.48; N, 4.95. Calcd for $C_{27}H_{63}N_9O_9I_9Pb_3Y$ (2510.5): C, 12.90; H, 2.50; N, 5.01%. ν_{max}(Nujol)/cm^{-1} 1654s (C═O), 1249m, 1111s, 1052m, 681s, 400s (Y−O). δ_H(300 MHz; CD_3CN) 2.81 (24 H, s, *trans* Me), 2.95 (24 H, s, *cis* Me), 7.98 (8 H, s, CHO).

$[Y(DMSO)_8]_2[(DMSO)_2Pb_5(\mu_3\text{-}I)_2(\mu\text{-}I)_8I_6]$ (2a). Using the above procedure, **2** was obtained by the reaction of a DMSO solution of PbI_2 (1.35 g, 2.32 mmol) and NH_4I (2 mL, 3.5 M) with $YI_3(Pr^iOH)_4$ (0.55 g, 0.77 mmol) in DMSO, followed by crystallization at room temperature by placing a toluene (3 mL) layer on the DMSO solution (3 mL). Yield, 1.27 g (71%). Anal. Found: C, 9.24; H, 2.29. Calcd for $C_{36}H_{108}I_{16}O_{18}Pb_5S_{18}Y_2$ (4650.6): C, 9.29; H, 2.32%. ν_{max}(Nujol)/cm^{-1} 995s (S−O), 952s, 675w, 415s (Y−O). δ_H (300 MHz; CD_3CN) 2.56 (108 H, s, Me_2S).

$[Y(DMSO)_8][Y(DMSO)_7(DMF)][(DMSO)_2Pb_5(\mu_3\text{-}I)_2(\mu\text{-}I)_8I_6]$ (2b). Dissolution of **1** (1.12 g, 0.45 mmol) in DMSO (3 mL), followed by a carefully layering with toluene (3 mL) at room temperature gave **2b** as orange-yellow crystals. Yield, 0.69 g (67%). Anal. Found: C, 9.54; H, 2.32; N, 0.28. Calcd for $C_{37}H_{109}NI_{16}O_{18}Pb_5S_{17}Y_2$ (4645.7): C, 9.55; H, 2.34; N, 0.30%. ν_{max}(Nujol)/cm^{-1} 1651m (C═O), 1000s (S−O), 954s, 900m, 674m, 422s (Y−O). δ_H (300 MHz; CD_3CN) 2.60 (102 H, s, Me_2S), 2.80 (3 H, s, *trans* Me), 2.93 (3 H, s, *cis* Me), 7.90 (1 H, s, CHO). Recrystallization of **1** under slightly differently different conditions, that is, from concentrated DMSO solution alone, gave crystals of **2a** in moderate yield (37%).

$[Y(DMF)_6(H_2O)_2][Pb_3(\mu_3\text{-}I)(\mu\text{-}I)_7I]_{1\infty}$ (3). Crystals of **1** (0.3 g, 0.12 mmol) transformed into yellow colored **3** within two weeks time of leaving in the paratone and were isolated and washed repeatedly with cold *n*-pentane (3−4 times). Yield, 0.18 g (65%). Anal. Found: C, 9.27; H, 1.78; N, 3.63. Calcd for $C_{18}H_{42}N_6O_8I_9Pb_3Y$ (2323.2): C, 9.29; H, 1.80; N, 3.61%. ν_{max}(Paratone)/cm^{-1} 3342br (O−H), 1650s (C═O), 1602w, 1582w (δ O−H), 1249m, 1111s, 1052m, 681s, 400s (Y−O). Poor solubility of **3** in commonly used NMR solvents precluded its characterization by ^1H NMR spectroscopy.

$[Y(DMSO)_7][Pb_3(\mu_3\text{-}I)(\mu\text{-}I)_7I]_{1\infty}$ (4). On leaving in the paratone, crystals of **2b** (0.47 g, 0.10 mmol) transform into **4** in 2−3 weeks time. These yellow-colored crystals were isolated from paratone

Table 1. Crystallographic and Refinement Data of **1**−**4**

compound	**1**	**2a**	**2b**	**3**	**4**
empirical formula	$C_{24}H_{56}N_8O_8Y.Pb_3I_9\cdot C_3H_7NO$	$C_{36}H_{108}O_{18}S_{18}Y_2\cdot Pb_5I_{16}$	$C_{37}H_{109}NO_{18}S_{17}Y_2\cdot Pb_5I_{16}$	$C_{18}H_{42}N_6O_8Y\cdot Pb_3I_9$	$C_{28}H_{84}O_{14}S_{14}Y_2\cdot Pb_6I_{18}$
formula weight	2510.50	4650.71	4645.67	2323.21	4799.18
crystal system	orthorhombic	triclinic	monoclinic	monoclinic	triclinic
space group	*Pcab*	$P\bar{1}$	$P2_1/c$	$P2_1/n$	$P\bar{1}$
a (Å)	22.1948(4)	10.8903(4)	21.0292(2)	10.4355(5)	15.2810(5)
b (Å)	23.6739(4)	15.6006(4)	15.7685(2)	18.4559(9)	17.5643(5)
c (Å)	24.0851(3)	17.8810(6)	35.7960(4)	27.2727(7)	19.4559(7)
α (deg)	90	96.196(2)	90	90	95.739(2)
β (deg)	90	97.805(2)	98.4301(6)	100.737(3)	94.6285(2)
γ (deg)	90	90.086(2)	90	90	93.4272(2)
volume (Å^3)	12655.2(4)	2991.8(2)	11741.7(2)	5160.7(4)	5166.7(3)
Z	8	1	4	4	2
M (mm^{-1})	13.30	12.45	12.67	16.29	16.55
temperature (K)	150	150	150	150	150
unique data (R_{int})	15050 (0.039)	13086 (0.100)	27517(0.181)	8761 (0.086)	23906 (0.040)
data/restrains/ parameters	8257/0/523	4582/144/440	13994/18/865	4161/108/409	16388/0/739
goodness of fit	1.05	1.10	1.10	1.12	1.02
R_1 ($I > 2(\sigma)$)	0.0385	0.0575	0.0534	0.0497	0.0446
R_1 (all data)	0.0859	0.1768	0.0910	0.1239	0.0771
wR_2 ($I > 2(\sigma)$)	0.0442	0.0588	0.0608	0.0548	0.0515
wR_2 (all data)	0.0814	0.1951	0.0736	0.1287	0.0944
residual electron density (e Å^{-3})	−1.71 to 3.95	−1.61 to 3.97	−2.95 to 2.59	−2.09 to 2.06	−2.05 to 2.20

and washed repeatedly with cold *n*-pentane (3−4 times). Yield, 0.23 g (48% wrt yttrium). Anal. Found: C, 7.10; H, 1.74. Calcd for $C_{14}H_{42}I_9O_7Pb_3S_7Y$ (2399.6): C, 7.00; H, 1.75%. ν_{max}(Nujol)/cm^{-1} 1000s (S−O), 955s, 674w, 418s (Y−O). δ_H (300 MHz; CD_3CN) 2.58 (84 H, s, Me_2S).

Attempted synthesis of **4** in solution phase by the reaction of **2b** (0.39 g, 0.08 mmol) and PbI_2 (0.05 g, 0.08 mmol) in DMSO (3 mL) followed by crystallization via layering this DMSO solution (3 mL) with toluene (5 mL) at room temperature gave orange-yellow crystals (0.4 g), the elemental analysis and single crystal unit cell determination studies showing them to be **2a**.

X-ray Crystallography. Crystals of **1**−**4** were obtained as mentioned above and mounted on a Nonius Kappa CCD diffractometer using Mo K_λ radiation ($\lambda = 0.71073$ Å). Intensities were collected at 150 K by means of the COLLECT software.[17] Reflection indexing, Lorentz-polarization correction, peak integration, and background determination were carried out with DENZO.[18] Frame scaling and unit-cell parameters refinement were made with SCALEPACK.[18] An analytical absorption correction was applied using the modeled faces of the crystal.[19] The structures were solved by direct methods with SIR97.[20] The remaining non-hydrogen atoms were located by successive difference Fourier map analyses. H-atoms were placed geometrically and included in the refinement using soft restraints on the bond lengths and angles to regularize their geometry (C−H in the range 0.93−0.98 Å and O−H = 0.82 Å) and isotropic atomic displacement parameters (*U*(H) in the range 1.2−1.5 times $U_{eq.}$ of the adjacent atom). In the last cycles of the refinement, the hydrogen atoms were refined using a riding mode. The structure refinement was carried out with CRYSTALS.[21] Crystallographic and refinement data for **1**−**4** are given in Table 1. For crystallographic data in CIF or other electronic format see the Supporting Information.

Results

(i) Synthesis. Reactions of solvated yttrium iodide precursors $[Y(L)_8]I_3$ (L = DMF or DMSO),[22] prepared in situ by stirring $YI_3(Pr^iOH)_4$ in DMF or DMSO at room temperature, with 3 equiv of lead(II) iodide in the presence of a 3.5 M solution of NH_4I in DMF/DMSO resulted in yellow colored clear solutions, from which derivative $[Y(DMF)_8][Pb_3I_9]_{1\infty}\cdot$DMF (**1**) and $[Y(DMSO)_8]_2[Pb_5I_{16}(DMSO)_2]$ (**2a**) were crystallized by cooling the DMF solution at −20 °C and layering the DMSO solution with toluene at room temperature, respectively (Scheme 1). Dissolution of **1** in DMSO, followed by a careful layering of this solution with toluene (1:1 ratio) at room temperature gave mixed-solvate complex $[Y(DMSO)_8][Y(DMSO)_7(DMF)][Pb_5I_{16}(DMSO)_2]$ (**2b**) in 67% yield. On the other hand, crystallization of **1** from the concentrated DMSO solution alone yielded **2a** with moderate yield (37%). The formation of different structural forms of iodoplumbates on using DMF or DMSO solvents can be attributed to different coordinating ability of these ligands toward lead metal. Obviously, the formation of $[(DMSO)_2Pb_5I_{16}]^{6-}$ cluster in **2a** and **2b** is caused by the presence of DMSO molecules on two terminal lead atoms of the above discrete cluster, which results in a saturated coordination sphere of those Pb atoms and thus cutting short the 1D structure of $[Pb_3(\mu\text{-}I)_9]$ chain (in **1**) in a discrete pentanuclear iodoplumbate cluster (in **2a** and **2b**). On leaving in the paratone (a low temperature cryoprotactant for X-ray crystallography), crystals of **1** transform in two to three weeks time into $[Y(DMF)_6(H_2O)_2][Pb_3I_9]_{1\infty}$ (**3**) via substitution of two DMF ligands by water molecules, whereas those of **2a** and **2b** are converted into $[Y(DMSO)_7][Pb_3I_9]_{1\infty}$ (**4**) via a decomposition reaction that also involves removal of one DMF and/or DMSO molecules from two yttrium cations and two DMSO molecules

(17) Nonius, B. V. *COLLECT*; Nonius: Delft, The Netherlands, 1997−2001.
(18) Otwinowski, Z.; Minor, W. *Methods in Enzymology*; Carter, C. W., Jr., Sweet, R. M., Eds.; Academic Press: New York, 1997; Vol. *276*, pp 307−326.
(19) De Meulenaar, J.; Tompa, H. *Acta Crystallogr.* **1965**, *A19*, 1014–1018.
(20) Altomare, A.; Burla, M. C.; Camalli, M.; Cascarano, G. L.; Giacovazzo, C.; Guagliardi, A.; Moliterni, A. G. G.; Polidori, G.; Spagna, R. *J. Appl. Crystallogr.* **1999**, *32*, 115–119.
(21) Watkin, D. J.; Prout, C. K.; Pearce, L. J. *CAMERON*; Chemical Crystallography Laboratory: Oxford, U.K., 1996.
(22) (a) Abbas, A.; Risberg, E. D.; Eriksson, L.; Mink, J.; Persson, I.; Sandstrom, M.; Sidorov, Y. V.; Skripkin, M. Y.; Ullstrom, A.-S. *Inorg. Chem.* **2007**, *46*, 7731–7741. (b) Berthet, J.-C.; Thuery, P.; Ephritikhine, M. *Polyhedron* **2006**, *25*, 1700–1706. (c) Lindqvist-Reis, P.; Naslund, J.; Persson, I.; Sandstrom, M. *J. Chem. Soc., Dalton Trans.* **2000**, 2703–2710.

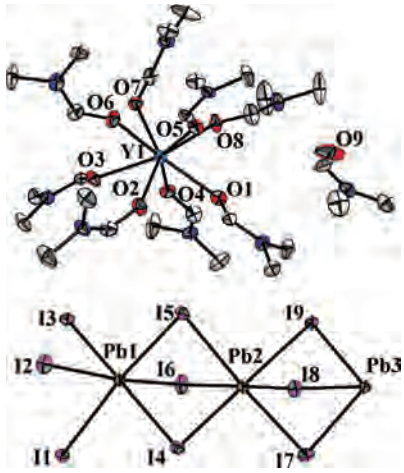

Figure 1. ORTEP structure of **1** with atom labeling and ellipsoids at 30% probability. Hydrogen atoms are omitted for clarity.

from $[Pb_5I_{16}(DMSO)_2]^{3-}$ cluster, as well as condensation of this discrete pentanuclear cluster into a zigzag 1D chain. Crystals of **3** and **4** can be conveniently isolated from paratone by repeatedly washing with cold *n*-pentane (3−4 times) and used for elemental analysis, spectroscopic, and thermal studies. These yellow or orange-yellow air-stable complexes **1**−**4** show good solubility in high polar solvents such as DMF and DMSO but are poorly soluble in common organic solvents. Except for **3**, they are moderately soluble in acetonitrile, thus allowing them to be characterized additionally by ^{1}H NMR spectroscopy.

(ii) X-ray Structures. The structure of **1** is composed of $[Y(DMF)_8]^{3+}$ cations and a 1D iodoplumbate chain with face sharing trioctahedral $[Pb_3(\mu\text{-}I)_9]^{3-}$ as the building unit (Figure 1). The eight-coordinate yttrium atom in the cation $[Y(DMF)_8]^{3+}$ has a distorted square antiprismatic geometry.[23] Similar stereochemistry has been found in many other 8-coordinate yttrium/lanthanide compounds.[13−15] The Y−O bond distances, varying from 2.285(6) to 2.411(7) Å, are also comparable to those observed for other 8-coordinate yttrium cations.[13−15,22] The inorganic motif is built up from characteristic face-sharing PbI_6 octahedra that form infinite straight chains along the *c*-axis (Figure 2a). Adjacent octahedra are joined by common faces (I1/I2/I3, I4/I5/I6, and I7/I8/I9) and are distorted with all lead iodide distances being different, ranging from 3.134(9) to 3.345(9) Å. The bond angles between *cis* ligands vary from 81.6(2)° to 102.3(3)° and *trans* angles from 170.2(8)° to 176.7(2)° (Table 2). The yttrium cations are arranged in a net-like structure along the *ab* plane, with channels in between being occupied by iodoplumbate chains running along the *c* axis (Figure 2b). However, there are no significant hydrogen-bonding interactions either among the yttrium cations or between yttrium cations and iodoplumbate chains.

The structures of **2a** and **2b** are similar except that in **2a** there is only one kind of yttrium cation, that is, $[Y(DMSO)_8]^{3+}$, and with only three crystallographically independent Pb atoms, the $[(DMSO)_2Pb_5I_{16}]^{6-}$ anion is more symmetric. Only the **2b** structure is discussed here (Table 3), whereas Oak Ridge Thermal Ellipsoid Plot (ORTEP) and packing diagrams (Figures S1 and S2) as well as some selected bond lengths and angles (Table S1) of **2a** are given in the Supporting Information. Compound **2b** has two types of 8-coordinate yttrium cations, $[Y(DMSO)_8]^{3+}$ and $[Y(DMSO)_7(DMF)]^{3+}$, the latter having a more regular square antiprismatic stereochemistry than the former (Figure 3).[23] The Y−O distances range from 2.297(1) to 2.398(1) Å, the Y−O(DMF) distance, 2.379(1) Å, being slightly longer than the Y−O (DMSO) distance (av. 2.349 Å). The charge balance for these two yttrium cations is provided by a pentanuclear $[(DMSO)_2Pb_5(\mu_3\text{-}I)_2(\mu\text{-}I)_8I_6]^{6-}$ anion (Figure 3). The characteristic face-sharing $PbI_6/PbOI_5$ octahedra form the structure of this $Pb_5I_{16}^{6-}$ anion, which can be viewed as built up from two Pb_2 units connected by a PbI_6 polyhedron. The $[Pb(1)OI_5]/[Pb(5)OI_5]$ and $[Pb(2)I_6]/[Pb(4)I_6]$ octahedra connect through a common face [I3I4−I5]/[I11−I13−I14] to form two dimers, which in turn, are connected through $[Pb(3)I_6]$ via two common trans faces [I4, I7, I8]/[I9, I10, I11] to form a zigzag anion (Figure 4). As a consequence of the connectivity of $[PbI_6]/[PbOI_5]$ octahedra, the iodide ligands act as either triply bridging (I4, I11), doubly bridging (I3, I5, I7, I8, I9, I10, I13, I14), or terminal ligands (I1, I2, I6, I12, I15, I16), the average Pb−I bond distances decreasing gradually from 3.394 to 3.265 and 3.099 Å for μ_3-I, μ-I, and terminal-I, respectively. The Pb−O(DMSO) and Pb···Pb distances, 2.496(1)−2.535(1) and 4.073(1)−4.202(1) Å, respectively, compare well with those in the literature.[5b,6c,7g] The $[(DMSO)_2Pb_5(\mu_3\text{-}I)_2(\mu\text{-}I)_8I_6]^{6-}$ anion reported here is unprecedented and very different from the only other known discrete pentanuclear iodoplumbate $[Pb_5(\mu_5\text{-}I)(\mu\text{-}I)_{10}I_5]^{6-}$ anion consisting of a cyclic arrangement of five PbI_2 octahedra and sharing one common iodide anion in the center of an almost planar Pb_5 ring.[24] It is also worth mentioning that structures of most of the Pb−I hybrid derivatives consist of 1-, 2- or 3D extended arrays,[7] and only few reports on discrete iodoplumbate anions are available including a recently reported mixed oxo-alkoxo-iodide derivative $[Pb_7(O)_2(OMe)_4I_6]$.[6,24,25]

Partial substitution of the DMF ligands of the $[Y(DMF)_8]^{3+}$ cation of **1** by water molecules in paratone after two to three weeks afforded a mixed-ligand cation $[Y(DMF)_6(H_2O)_2]^{3+}$ where the metal has also a distorted square antiprismatic stereochemistry (Figure 5). The Y−O (H_2O) bond distances (2.396 Å av.) are slightly longer than the Y−O (DMSO) ones (2.332 Å av.) as observed previously for other mixed ligand H_2O-DMSO complexes.[13,14] Although compositionally the building block of the iodoplumbate chain remains $[Pb_3I_9]^{3-}$, the presence of water molecules in the yttrium cation introduces H-bonding between iodides and water molecules, which transforms a straight Pb−I chain of **1** in to a zigzag chain [angle slightly over 90 °] (Figure 6a). From a structural point of view, this chain can be considered as built-up from two types of trimers arranged alternatively via doubly

(23) (a) Haigh, C. W. *Polyhedron* **1995**, *14*, 2871–2878. (b) Haigh, C. W. *Polyhedron* **1996**, *15*, 605–643.

(24) Krautscheid, H.; Vielsack, F. *Z. Anorg. Allg. Chem.* **2000**, *626*, 3–5.

(25) Shi, Y.-J.; Xu, Y.; Chen, X.-T.; Xue, Z; You, X.-Z. *Eur. J. Inorg. Chem.* **2002**, 3210–3213.

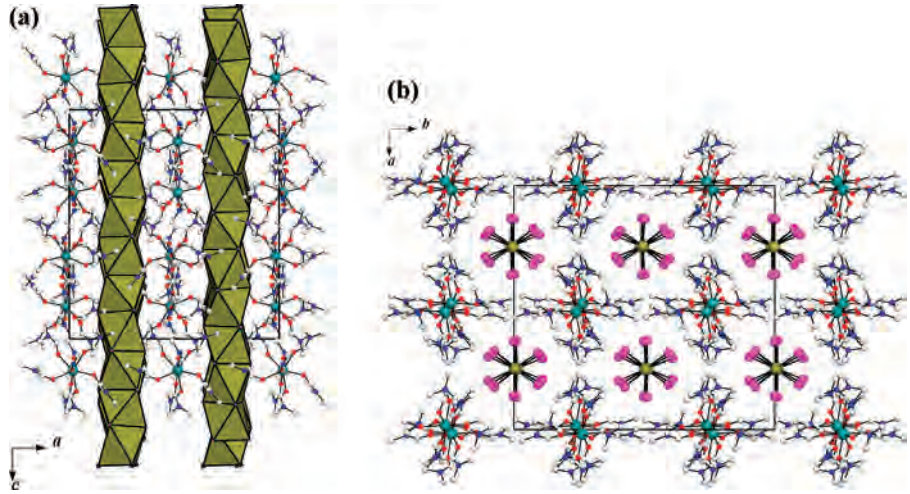

Figure 2. View of **1** along *b* axis (a) and *c* axis (b).

Table 2. Selected Bond Lengths (Å) and Angles (deg) for **1**

Bond Length			
Pb1—I1	3.2425(8)	Pb3—I7	3.3458(9)
Pb1—I2	3.3262(9)	Y1—O8	2.329(6)
Pb1—I3	3.1910(9)	Y1—O1	2.364(7)
Pb1—I4	3.2893(9)	Y1—O4	2.285(6)
Pb1—I5	3.2119(8)	Y1—O7	2.328(7)
Pb1—I6	3.1520(8)	Y1—O6	2.359(6)
Pb2—I4	3.1956(9)	Y1—O5	2.332(6)
Pb2—I5	3.2309(8)	Y1—O3	2.411(7)
Pb2—I6	3.2891(8)	Y1—O2	2.301(7)
Bond Angle			
I4—Pb1—I3	172.71(2)	O8—Y1—O6	120.9(3)
I4—Pb1—I2	102.37(3)	O1—Y1—O6	137.6(2)
I3—Pb1—I2	83.93(3)	O4—Y1—O6	143.7(2)
I4—Pb1—I6	87.30(3)	O7—Y1—O6	74.2(3)
I3—Pb1—I6	86.35(2)	O8—Y1—O5	75.8(2)
I2—Pb1—I6	170.28(2)	O1—Y1—O5	73.9(2)
I3—Pb1—I5	98.05(3)	O4—Y1—O5	144.1(2)
I2—Pb1—I5	97.14(2)	O7—Y1—O5	108.6(2)
I6—Pb1—I5	84.51(2)	O8—Y1—O3	135.2(2)
I3—Pb1—I1	88.59(3)	O1—Y1—O3	126.8(2)
I2—Pb1—I1	84.06(2)	O8—Y1—O2	146.0(3)
I6—Pb1—I1	95.41(3)	O4—Y1—O2	102.8(3)
I5—Pb1—I1	173.34(2)	O7—Y1—O2	142.7(2)
O8—Y1—O1	72.6(2)	O6—Y1—O2	79.3(3)
O8—Y1—O4	77.3(3)	O5—Y1—O2	87.0(3)
O1—Y1—O4	75.6(2)	O1—Y1—O7	141.6(2)
O8—Y1—O7	71.2(3)		

Table 3. Selected Bond Lengths (Å) and Angles (deg) for **2b**

Bond Length			
Pb1—I1	3.137(1)	Pb3—I8	3.220(1)
Pb1—I2	3.099(1)	Pb3—I9	3.250(1)
Pb1—I3	3.212(1)	Pb3—I10	3.201(1)
Pb1—I4	3.386(1)	Pb3—I11	3.239(1)
Pb1—I5	3.455(1)	Y2—O9	2.321(1)
Pb1—O17	2.496(1)	Y2—O10	2.398(1)
Pb2—I3	3.384(1)	Y2—O11	2.359(9)
Pb2—I4	3.450(1)	Y2—O12	2.363(1)
Pb2—I5	3.289(1)	Y2—O13	2.323(9)
Pb2—I6	3.048(1)	Y2—O14	2.375(1)
Pb2—I7	3.208(1)	Y2—O15	2.297(1)
Pb2—I8	3.236 (1)	Y2—O16	2.379(1)
Pb3—I4	3.236(1)		
Bond Angle			
I4—Pb1—I1	171.82(3)	I3—Pb2—I8	163.75(3)
I2—Pb1—I1	99.84(3)	I4—Pb3—I11	174.58(3)
I4—Pb1—O17	81.8(3)	I11—Pb3—I10	85.42(3)
I1—Pb1—O17	91.8(3)	I11—Pb3—I8	99.56(3)
I2—Pb1—I5	167.77(3)	I9—Pb3—I8	173.93(3)
O17—Pb1—I5	86.5(3)	I10—Pb3—I8	100.37(3)
I2—Pb1—I3	97.40(3)	O15—Y2—O13	105.7(4)
O17—Pb1—I3	166.8(3)	O13—Y2—O9	141.3(3)
I4—Pb2—I6	171.86(3)	O14—Y2—O9	145.0(4)
I4—Pb2—I7	80.81(3)	O13—Y2—O11	83.7(4)
I6—Pb2—I7	93.73(3)	O15—Y2—O10	145.8(3)
I6—Pb2—I5	100.66(3)	O13—Y2—O10	80.4(4)
I7—Pb2—I5	165.45(3)	O14—Y2—O10	137.4(3)
I6—Pb2—I3	103.19(3)	O11—Y2—O10	70.6(3)
I7—Pb2—I3	88.34(3)	O14—Y2—O16	122.2(4)
I5—Pb2—I8	98.04(3)		

and triply bridging iodides. Out of four crystallographically independent Pb atoms present in the slightly distorted [PbI_6] octahedral coordination environment, two [Pb(3)I_6] and one [Pb(4)I_6] octahedra connect through common trans faces [I7−I8−I9] to form the first trimer, whereas the second trimer is composed of two [Pb(2)I_6] and one [Pb(1)I_6] octahedra also connected through common trans faces [I1−I2−I6]. The Pb4 and Pb1 atoms of these trimers are on inversion centers (Figure 5). These two timers are then joined by one triply bridging iodide I6 and two double-bridging iodides I4 and I5 to form a wave-shape anion chain extending along the *b* axis (Figure 6a). The iodide ligands in this chain are in either bridging (μ_3 and μ) or terminal positions, the average Pb−I bond distances increase from 3.013 to 3.245 and 3.300 Å as the connectivity of iodides increases from one to three (Table 4). The Pb···Pb distances range from 4.050(1) −4.202(1) Å. This zigzag iodoplumbate chain represents a new structural motif and isomeric form of the known 1D iodoplumbate chain.[7] The presence of two water molecules on the cation introduces trifurcated H-bonding with I···O(H_2O) distances ranging from 3.50(1) to 3.89(2) Å (Figure 5). These distances are in agreement with those reported for hydrogen bonding involving iodides.[13,26] Because of the angle 82.0(6)° between the water molecules, the yttrium cations act as templates for the bending and formation of the pockets of the anionic Pb−I chain. These yttrium cations occupy alternate positions along the zigzag Pb−I chain, and the overall structure of **3** is a 1D zigzag polymer (Figure 6a). This extended structure of **3** can be compared with the recently published zigzag

(26) Fromm, K. M. *Chem.—Eur. J.* **2001**, *7*, 2236–2244.

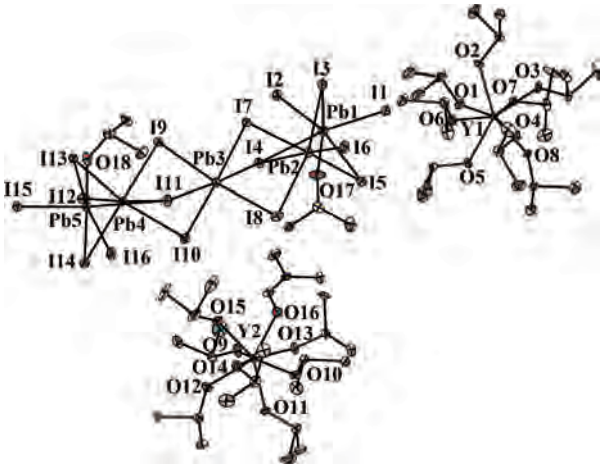

Figure 3. ORTEP structure of **2b** with atom labeling and ellipsoids at 30% probability. Hydrogen atoms are omitted for clarity.

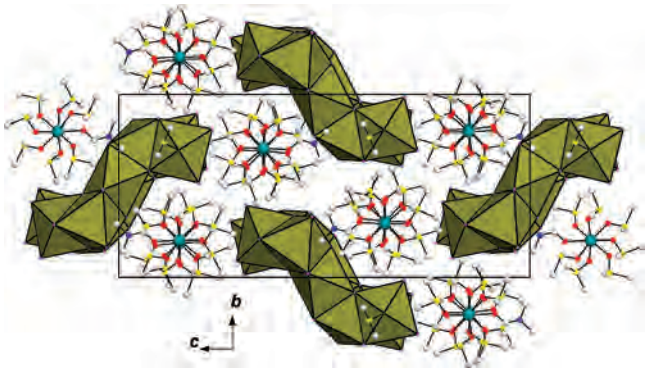

Figure 4. View of **2b** along *a* axis.

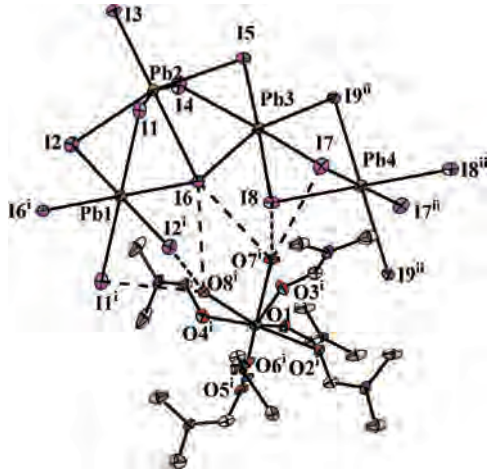

Figure 5. ORTEP structure of **3** showing trifurcate H-bonding between water molecules on yttrium cation and iodides of iodoplumbate anions (ellipsoids at 30% probability). Hydrogen atoms are omitted for clarity. H-bonding between water molecules and iodides are shown as broken lines: $I1^{i}\cdots O8^{i}$ 3.51(2); $I2^{i}\cdots O8^{i}$ 3.56(2); $I6\cdots O8^{i}$ 3.89(2); $I6\cdots O7^{i}$ 3.76(2); $I7\cdots O7^{i}$ 3.75(2); $I8\cdots O7^{i}$ 3.50(1) Å; symmetry codes: (i) $^{1}/_{2} + x$, $^{1}/_{2} - y$, $z - {}^{1}/_{2}$; (ii) $^{1}/_{2} - x$, $^{1}/_{2} + y$, $^{1}/_{2} - z$.

iodocuperate chain also templated by the $[Y(DMF)_6(H_2O)_2]^{3+}$ cation.[13]

On leaving in paratone for 2−3 weeks, crystals of **2a** and **2b** are converted into $[Y(DMSO)_7][Pb_3(\mu_3\text{-}I)(\mu\text{-}I)_7I]_{1\infty}$ (**4**) via a decomposition pathway involving removal of one solvent molecule (DMF or DMSO) from each yttrium cation, two DMSO molecules from the $[Pb_5I_{16}(DMSO)_2]^{3-}$ cluster, as well as condensation of this discrete pentanuclear cluster into a zigzag 1D chain. The tendency of the $[YL_8]^{3+}$ (L = DMSO and DMF) cation to lose or replace one or more ligands has previously been demonstrated.[13−15] In contrast to the structures of **1**−**3**, yttrium centers are 7-coordinated here and have a slightly distorted pentagonal bipyramidal geometry (Figure 7). Because of the lower coordination number of yttrium, the average Y−O (DMSO) bond distance, 2.298 Å, is shorter than those in **2a** and **2b**. The iodoplumbate chain of **4** is structurally identical to the zigzag Pb−I chain of **3** (Figure 8a). The Pb−I (μ_3-, μ- or terminal) bond lengths and Pb···Pb distances are also almost the same as those found in **3** (Table 5). However, in the absence of water molecules on yttrium cations, there are no H-bonding interactions between metal-organic cations and iodoplumbate chains in **4**. The spatial arrangement of $[Y(DMSO)_7]^{3+}$ cations around the 1D iodoplumbate chain is also different in **4**. So unlike in **3**, where the yttrium cations occupy alternate semipocket positions along the zigzag Pb−I chain (because of trifurcate H-bonding between O—I, Figure 6b), the iodoplumbate chain in **4** is surrounded by yttrium cations in four directions forming a sort of net (Figure 8b). The overall crystal packing of **4** can be compared with the pseudo body-centered cubic packing (e.g., CsI), with Y atoms occupying the corners of the cube and the Pb3 being in the center (Figure 8b).

(iii) Thermo-Gravimetric Studies. To examine the thermal stabilities of the complexes **1**−**4**, TG-DTA studies were carried out in air in the temperature range 20−600 °C, and some selected data such as decomposition stages, temperature, total weight loss, positions of endo- and exothermic peaks, and so forth are summarized in Supporting Information, Table S2. The TGA curves of these complexes show a two-to-four stage decomposition process and indicate that thermal stability decreases in the order: **3** > **1** > **4** > **2b** (Figure 9). The extraordinary stability of the mixed DMF-H_2O ligand complex **3** can be attributed to the presence of strong H-bonds between H_2O and some of I^- ligands. For these complexes, the decomposition temperatures as well as total percentage weight loss vary in the 450−520 °C and 57.8−65.5% ranges, respectively. The decomposition pattern can be generalized by saying that the first two decomposition stages of **1**−**3** (first stage in case of **4**) are accompanied by the loss of solvate molecule of crystallization, water molecules, and DMF/DMSO molecules on yttrium cations and lead-iodide clusters, as supported by strong endothermic peaks in DTA curves (Supporting Information, Figure S3). Further heating of the complexes is accompanied by the loss of iodide contents as HI from the iodoplumbate moieties as supported by strong exothermic peaks in the 290−520 °C temperature range. This pattern of decomposition is quite similar to that reported recently by us for iodocuperate derivatives templated by metal-organic yttrium complexes, where the loss of iodide contents as HI in the 160−460 °C temperature range was supported by mass spectrometry.[13]

(iv) Spectroscopic Characterization. The FT-IR and ^{1}H NMR spectra of **1**−**4** are simple and show characteristic absorptions/peaks due to the coordinating ligands on the yttrium cation. The FT-IR spectra of the complexes containing DMF

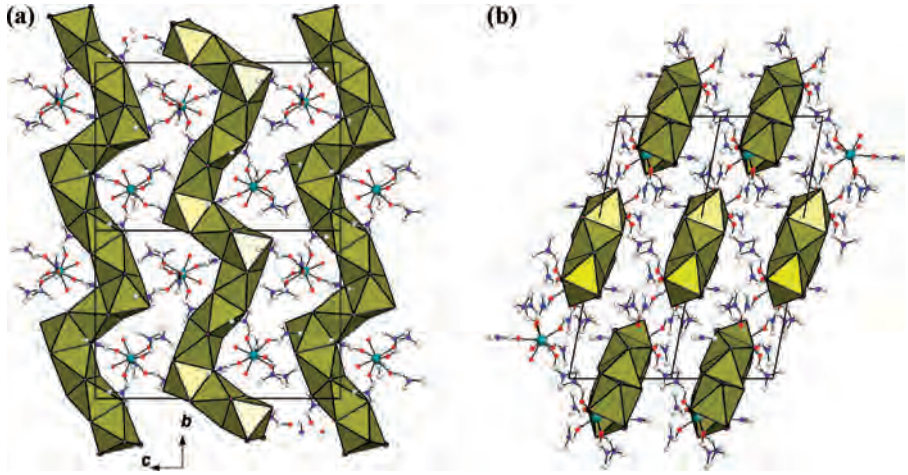

Figure 6. View of **3** along *a* axis (a) and *b* axis (b).

Table 4. Selected Bond Lengths (Å) and Angles (deg) for **3**

	Bond Length		
Pb1—I1	3.259(2)	Pb3—I7	3.149(2)
Pb1—I6	3.193(2)	Pb4—I8	3.275(2)
Pb2—I5	3.242(2)	Pb4—I7	3.195(2)
Pb2—I4	3.192(2)	Y1—O5	2.316(2)
Pb2—I1	3.281(2)	Y1—O7	2.395(1)
Pb2—I2	3.343(2)	Y1—O2	2.322(1)
Pb2—I3	3.013(2)	Y1—O8	2.398(2)
Pb2—I6	3.450(2)	Y1—O3	2.368(2)
Pb3—I6	3.257(2)	Y1—O4	2.341(2)
Pb3—I4	3.359(2)	Y1—O1	2.326(2)
Pb3—I8	3.248(2)	Y1—O6	2.322(2)
	Bond Angle		
I1[a]—Pb1—I1	179.99(6)	I8—Pb3—I4	101.44(6)
I1[a]—Pb1—I6	94.47(5)	I7—Pb3—I4	165.08(5)
I1—Pb1—I2	84.03(6)	I6—Pb3—I4	88.02(5)
I6—Pb1—I2	87.44(5)	O2—Y1—O4	148.2(5)
I8[b]—Pb4—I8	179.99(6)	O8—Y1—O4	71.5(6)
I8[b]—Pb4—I7	92.31(6)	O3—Y1—O4	133.2(6)
I5—Pb2—I2	165.60(5)	O5—Y1—O1	79.3(6)
I5—Pb2—I3	96.46(6)	O7—Y1—O1	69.8(5)
I3—Pb2—I6	176.71(6)	O8—Y1—O1	138.9(6)
I5—Pb2—I4	80.47(6)	O3—Y1—O1	122.8(6)
I1—Pb2—I4	168.39(6)	O7—Y1—O6	142.1(6)
I2—Pb2—I4	98.71(6)	O4—Y1—O6	119.7(6)
I6—Pb2—I4	87.50(6)	O1—Y1—O6	141.9(5)
I5—Pb3—I8	177.35(5)	O7—Y1—O2	100.8(6)
I5—Pb3—I7	90.42(6)	O5—Y1—O8	115.8(6)
I7—Pb3—I6	81.29(6)	O7—Y1—O8	82.0(6)
I5—Pb3—I4	78.70(6)	O2—Y1—O8	140.3(6)

[a] Symmetry codes: $-x, -y, 1-z$. [b] Symmetry codes: $-x, -1-y, 1-z$.

ligands, that is, **1**, **2b**, and **3** show an intense ν(C═O) vibration at 1650−1654 cm^{-1}, which is 20−25 cm^{-1} lower than the value for free DMF (1674 cm^{-1}). The DMSO complexes **2a**, **2b**, and **4** also exhibit an intense ν(S−O) peak at lower frequency (995−1000 cm^{-1}) than the value for free DMSO (1056 cm^{-1}). In all these spectra, the ν(Y−O) frequency appears as medium-to-strong intensity absorptions in the 400−420 cm^{-1} region. A broad strong absorption at 3342 cm^{-1} due to ν(OH) and a weak intensity band at 1602 cm^{-1} due to δ(OH) also confirm the presence of water molecules in **3**. In the ^{1}H NMR spectra of **1** and **2b**, the coordinated DMF ligands show three singlets in a 3:3:1 intensity ratio at 2.80−2.81, 2.93−2.95, and 7.90−7.98 ppm corresponding to the *trans* and *cis* Me, and CHO groups, respectively, whereas those of DMSO ligands in **2a**, **2b**, and **4** appear as a singlet at 2.56−2.58 ppm. The derivative **3** is poorly soluble in commonly used NMR solvents including CD_3CN and hence could not be studied by ^{1}H NMR spectroscopy.

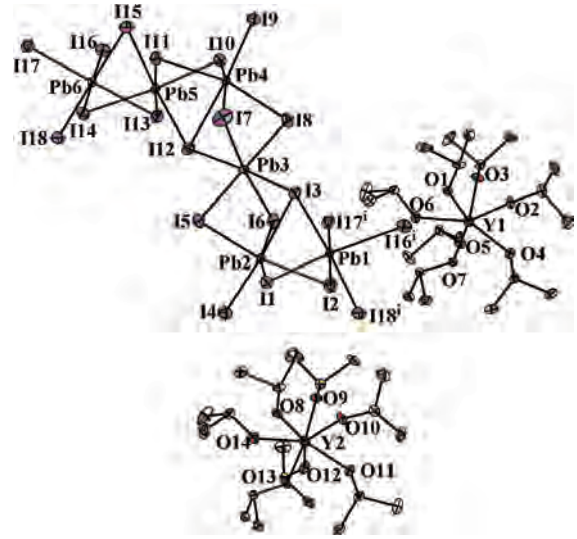

Figure 7. ORTEP structure of **4** with atom labeling and ellipsoids at 30% probability. Hydrogen atoms are omitted for clarity. Symmetry codes: (i) $x, y, z+1$.

UV−visible spectroscopy. The UV−visible spectral analysis of powder samples of **1**−**4** (diluted 3 times with SiO_2) were carried out at room temperature. Two broad peaks are found in the 488−515 nm and 380−430 nm ranges, the first one being characteristic of the corner, edge-, or face-sharing PbI_6 octahedra (Figure 10).[4a,5a,7l] A slight difference in the UV−vis spectra of **2a** and **2b** (similar $[(DMSO)_2Pb_5I_{16}]^{6-}$ anion) as well as **3** and **4** (similar zigzag $[Pb_3I_9]^{3-}$ chain) can be attributed to different interactions between yttrium cations and iodoplumbate anions arising because of their different spatial arrangement and the presence of strong H-bonding in **3**. Using diffuse-reflectance spectral analysis,[27] the optical band gap values of **1**−**4** were assessed to be in the 1.86−2.54 eV range (Figure 11 and Supporting Information, Figure S4). According to the Kubelka−Munk function: $F(R) = (1-R)^2/2R$, in which R is the experimentally observed reflectance, the BV-BC band gap is determined as the intersection point of the energy axis with the extrapolated

(27) Kortum, G. *Reflectance Spectroscopy Principles, Methods, Applications*; Springer-Verlag: New York, 1969.

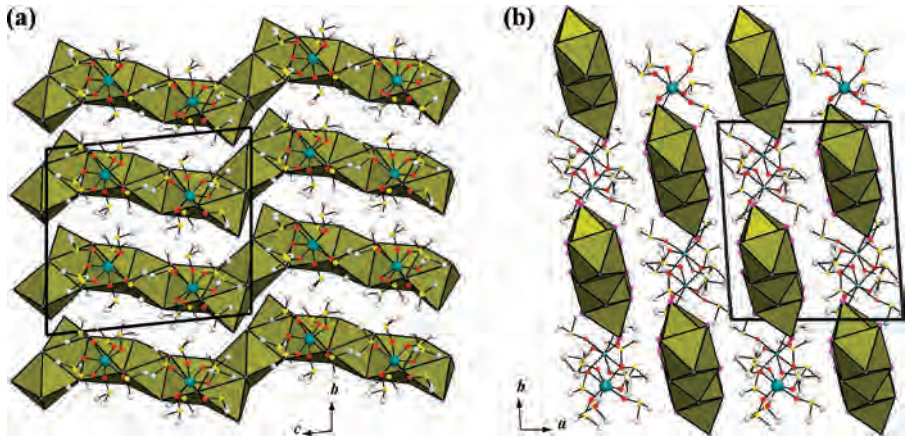

Figure 8. View of **4** along *a* axis (a) and *c* axis (b).

Table 5. Selected Bond Lengths (Å) and Angles (deg) for **4**

	Bond Length		
Pb1—I18[a]	3.1528(8)	Pb3—I7	3.1710(1)
Pb1—I17[a]	3.2552(8)	Pb3—I8	3.1607(8)
Pb1—I16[a]	3.4142(8)	Pb3—I3	3.2180(8)
Pb1—I2	3.2058(8)	Pb3—I12	3.2818(8)
Pb1—I3	3.2657(8)	Pb4—I12	3.6229(8)
Pb1—I1	3.0564(8)	Pb4—I7	3.2340(1)
Pb2— I2	3.2536(8)	Pb4—I8	3.2438(8)
Pb2—I5	3.1979(8)	Y1—O1	2.287(7)
Pb2—I6	3.1251(9)	Y1—O2	2.324(7)
Pb2—I4	3.0355(8)	Y1—O3	2.250(7)
Pb2—I1	3.4233(9)	Y1—O4	2.301(7)
Pb2—I3	3.5590(8)	Y1—O5	2.307(7)
Pb3—I5	3.2006(8)	Y1—O6	2.358(7)
Pb3—I6	3.2768(9)	Y1—O7	2.264(7)
	Bond Angle		
I18[a]—Pb1—I17[a]	89.85(2)	I5—Pb3—I8	176.18(2)
I17[a]—Pb1—I16[a]	82.44(2)	I6—Pb3—I3	85.05(2)
I18[a]—Pb1—I3	175.84(2)	I6—Pb3—I12	95.36(2)
I16[a]—Pb1—I3	99.23(2)	I8—Pb3—I12	89.21(2)
I2—Pb1—I3	90.78(2)	I3—Pb3—I12	175.84(2)
I18[a]—Pb1—I1	87.09(2)	O5—Y1—O7	96.4(3)
I16[a]—Pb1—I1	169.22(2)	O5—Y1—O6	72.6(3)
I2—Pb2—I5	166.43(2)	O7—Y1—O6	81.6(3)
I2—Pb2—I6	88.94(2)	O6—Y1—O4	139.5(2)
I2—Pb2—I4	100.49(2)	O7—Y1—O3	171.2(3)
I5—Pb2—I4	92.60(2)	O6—Y1—O3	90.1(3)
I4—Pb2—I1	99.93 (2)	O4—Y1—O3	106.9(3)
I2—Pb2—I3	84.98(2)	O7—Y1—O2	102.7(3)
I4—Pb2—I3	174.13(2)	O6—Y1—O2	146.5(3)
I1—Pb2—I3	78.62(2)	O4—Y1—O1	142.0(3)
I5—Pb3—I7	94.22(3)	O3—Y1—O1	88.0(3)
I6—Pb3—I7	173.50(3)		

[a] Symmetry code: $x, y, z - 1$.

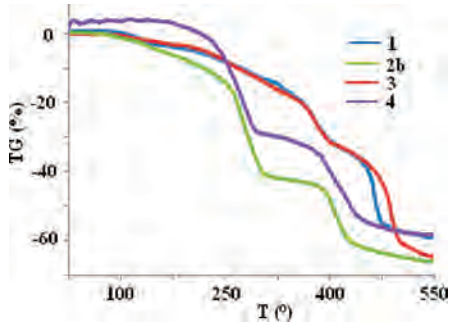

Figure 9. Thermo-gravimetric curves for **1**−**4**.

linear portion of the absorption edge in an $F(R)^2$ versus photon energy plot.[28] The band gap values obtained are

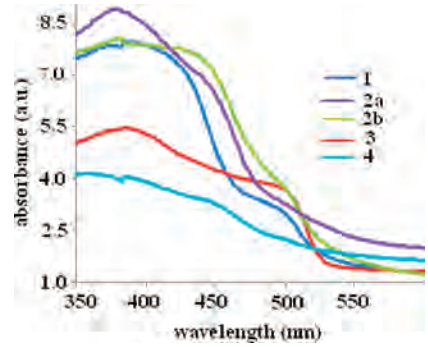

Figure 10. Room temperature UV−vis spectra of **1**−**4** in solid state.

similar to those usually associated to hybrid derivatives based on 1D and 2D iodoplumbates.[4a,7l]

(v) Luminescence Studies. Derivatives **1**, **2a**, and **2b** show intense luminescence at room temperature, whereas **3** and **4** are non-emissive (Figure 12). The excitation was corrected from the wavelength dependent emission of the Xenon lamp, which was measured independently with a Power meter. The intensity of the lamp being quite low below 280 nm, the spectra are rather noisy for the 200−280 nm wavelength range. When excited at 280 nm, the three derivatives **1**, **2a**, and **2b** exhibit emission maxima at 703 nm. Bulk excitation of the powder at 340 and above does not lead to luminescence. The luminescence is obtained through excitation deep into the gap of the material suggesting that it is a direct excitation of the iodine 5p-lead 6s to lead 6p charge transfer. A similar assignment has been suggested for some other hybrid iodoplumbates.[29] The non-emissive behavior of **3** and **4** may arise from the zigzag Pb−I chain structure with a Pb bridge enabling a stronger delocalization of the excitation, which can lead to quenching of the luminescence on defects.

Discussion

The auto-ionization of iodides in the precursor derivatives $[Y(L)_8]I_3$ (L = DMSO and/or DMF) was exploited for the template synthesis of hybrid iodoplumbate derivatives **1** and

(28) Cao, G.; Rabenberg, L. K.; Nunn, C. M.; Mallouk, T. E. *Chem. Mater.* **1991**, *3*, 149–156.
(29) (a) Fan, L.-Q.; Wu, L.-M.; Chen, L. *Inorg. Chem.* **2006**, *45*, 3149–3151. (b) Fan, L.-Q.; Huang, Y.-Z.; Wu, L.-M.; Chen, L.; Li, J.-Q.; Ma, E. *J. Solid State Chem.* **2006**, *179*, 2361–2366.

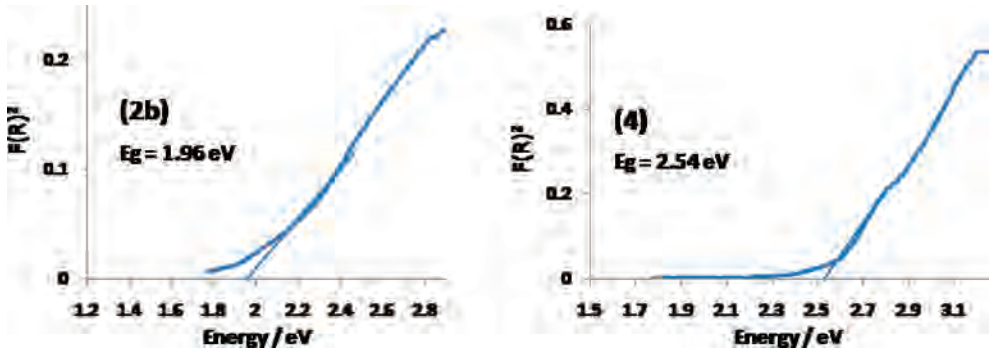

Figure 11. Diffuse reflectance spectra of **2b** and **4** in Kubelka−Munk units.

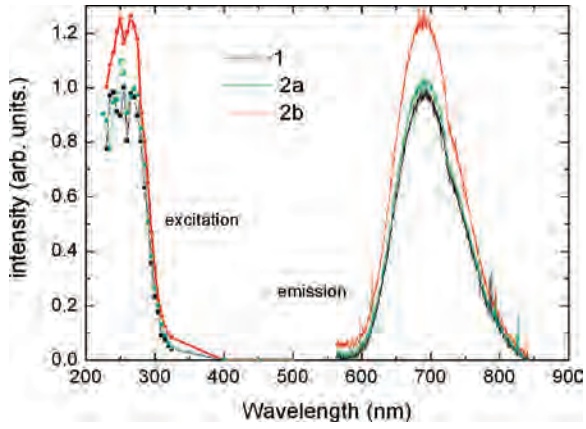

Figure 12. Room temperature solid state excitation and emission spectra of **1**, **2a**, and **2b**, all three showing emission maxima at 703 nm when excited at 280 nm.

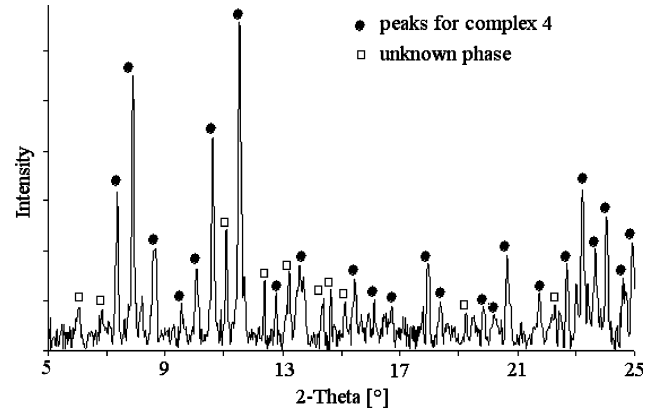

Figure 13. Powder X-ray pattern of **2a** after calcination at 140 °C for 2 h.

2a. The DMF molecules on yttrium cation of **1** can easily be replaced by DMSO or water molecules, in solution or solid phase, to afford new mixed-ligand hybrid derivatives **2b** and **3**, respectively. Like **1**, discrete complexes **2a** and **2b** also undergo solid-state transformation in a confined environment of paratone to give rise to another 1D polymer **4** based on zigzag iodoplumbate chains, the single crystallinity being maintained during the transformation. Entirely new structural motifs for hybrid iododplumbates such as those reported for **2a** and **2b** here are brought in by introducing metal organic cations. Moreover, by varying coordination number, geometry, and nature of the ligands within the metal-organic cations, a range of structures for iodoplumbate clusters, from a discrete pentanuclear unit in **2** to 1D straight and zigzag extended arrays in **1**, **3**, and **4** (Supporting Information, Figure S5), can be obtained and thus used to fine-tune the properties of these hybrid derivatives. For example, simply by choosing between DMSO or DMF ligand in the cation $[Y(L)_8]^{3+}$ (L = DMSO or DMF), two very different structures, a 1D straight chain polymer $[Pb_3(\mu\text{-}I)_9]_{1\infty}$ in **1** and a discrete pentanuclear $[(DMSO)_2Pb_5(\mu_3\text{-}I)_2(\mu\text{-}I)_8I_6]^{6-}$ in **2**, are obtained. Similarly, substitution of two DMF ligands with water molecules converts a straight Pb−I chain of **1** into a zigzag chain (complex **3**), the trifurcate H-bonding between water ligands on yttrium cation and iodide of the iodoplumbate anion playing a pivotal role in this transformation.

Whereas the above transformation of **1** to **3** is clearly an exchange reaction of solvent molecules on yttrium cation leading to reorganization of the 1D iodoplumbate chain, the conversion of **2a** and **2b** to **4** involves some decomposition as evidenced by a decrease in the yttrium-to-lead ratio during the transformation (0.40 in **2a** and **2b** vs 0.33 in **4**). Two hypotheses involving decomposition can be proposed for the solid-state transformation of **2a** and **2b** to **4**: (a) decomposition of a part of the pentanuclear iodoplumbate cluster in paratone to give some free PbI_2, which in turn react with remaining Pb_5I_{16} cluster to give zigzag chain of Pb_6I_{18} composition, and (b) departure of 1/6 of solvated yttrium cation together with DMSO molecules leading to the condensation of pentanuclear entities into a 1D zigzag chain. In spite of the uncertainty of the mechanism of decomposition, the removal of DMSO molecules from $[(DMSO)_2Pb_5I_{16}]^{6-}$ of **2a** and **2b**, resulting in an unsaturated coordination sphere of Pb atoms, appears to be the driving force for condensation of this pentanuclear unit to a 1D zigzag chain in **4**. To verify this, powder X-ray diffraction studies were performed on **2a** and **4** (Supporting Information, Figures S6 and S7) as well as the calcined sample of **2a** at 140 °C for 2 h (Figure 13). Indeed, the major component of the powder pattern obtained on the calcined sample corresponded to complex **4**, though an unknown minor phase was also present (Figure 13). That the removal of DMSO molecules from $[(DMSO)_2Pb_5I_{16}]^{6-}$ is really the decisive step for condensation of this pentanuclear unit is further corroborated by the fact that our efforts to mimic a similar transformation of **2** to **4** in solution phase by reacting **2b** with 1 equiv of PbI_2 in DMSO did not lead to the formation of a zigzag 1D iodoplumbate chain (Scheme 1).

Conclusion

We report in this paper a very simple, convenient, and high yield synthetic route for novel hybrid iodoplumbate derivatives templated by metal-organic complexes and describe their structural transformations, thermal, spectroscopic, and luminescent properties. The influence of solvated yttrium cations on the nuclearity and dimensionality of lead iodide clusters in **1**−**4**, varying from discrete pentanuclear units to straight and zigzag 1D extended arrays, as well as reaction and crystallization conditions leading to solid and solution phase transformations, is impressively shown here. New structural features are reported such as a novel pentanuclear $[(DMSO)_2Pb_5(\mu_3\text{-}I)_2(\mu\text{-}I)_8I_6]^{6-}$ anion in **2** and an hitherto unknown structural motif and isomeric form of $[Pb_3(\mu_3\text{-}I)(\mu\text{-}I)_7I]^{3-}$ building block of zigzag 1D iodoplumbate chains in **3** and **4**. This and other work from our laboratory[13,15] shows that use of metal-organic cations provides a better opportunity to fine-tune the properties of hybrid materials, simply by choosing a suitable coordinating ligand as well as varying coordination number, geometry, and oxidation state of the metal. Designing and generating robust supramolecular networks using anhydrous lanthanide halide complexes as precursors has remained largely unexplored.[30] We have previously shown[13,15] that ionized complexes of the $[Ln(L)_x]I_3$ (L = DMSO and/or DMF, $x = 7-9$) type has the potential to play an important role in generating iodide-mediated supramolecular frameworks and that the resulting metal complex-templated iodometallates are potential candidates as chemical sensors because of their sensitivity toward oxidation [e.g., Cu(I)] and different solvents as well as interesting supramolecular structures.

Acknowledgment. S.M. is grateful to the Centre National de la Recherche Scientifique (CNRS) for a postdoctoral fellowship. The help of M. Daniel for recording TG-DTA data is acknowledged.

Supporting Information Available: ORTEP and packing diagrams of **2a** (Figure S1 and S2), DTA curves for **1**−**4** (Figure S3), diffuse reflectance spectra of **1**, **2a,** and **3** in Kubelka−Munk units (Figure S4), three types of iodoplumbate anions reported in this paper (Figure S5), powder X-ray pattern of **2a** and **4** (Figure S6 and S7), selected bond lengths and angles for **2a** (Table S1), and selected TG-DTA data for **1**−**4** (Table S2). Five X-ray crystallographic files in CIF format. This material is available free of charge via the Internet at http://pubs.acs.org.

IC8010376

(30) Mishra, S. *Coord. Chem. Rev.* **2008**, *252*, 1996–2025.